J. Electrochem. Sci. Eng. **12(5)** (2022) 911-922; http://dx.doi.org/10.5599/jese.1333

Open Access : : ISSN 1847-9286
www.jESE-online.org

Original scientific paper

Comparison of erosion performance of uncladded and WC-based laser cladded SS304 and SS410 steels

Sarpreet Singh[1,✉], Parlad Kumar[1] and Deepak Kumar Goyal[2]

[1]*Punjabi University, Patiala, Punjab, India*
[2]*I. K. Gujral Punjab Technical University Jalandhar, Kapurthala, Punjab, India*

Corresponding author: ✉singh.sarpreet9976@gmail.com

Received: March 28, 2021; Accepted: June 3, 2022; Published: August 19, 2022

Abstract

Myriad hydro materials have been encountered with the severe attacks of eroded particles during the operation, leading to degradation of target material and economic loss. In this study, Colmonoy-6+WC powders were deposited with the help of the laser cladding method on the bare SS304 and SS410 steel surfaces. Distinct properties of cladded surfaces, such as mechanical as well as metallurgical properties, were investigated. The influence of slurry erosion parameters like angle of impact and impact velocity of eroded particles on the cladded as well as uncladded steel specimen was analysed. Under all slurry erosion conditions, there was an escalation in slurry erosion resistance in the case of cladded steel as that of as-received steel specimens. In slurry erosion, the influence of the impact velocity of erodent particles is more against the impact angle. The scanning electron microscopy images of eroded uncoated steel specimens represent ductile behaviour along with the formation lip, ploughing etc., while eroded cladded steels exhibit brittle behaviour.

Keywords

Ni+WC based coatings; erosive wear; laser cladding

Introduction

In this contemporary era, there is a plethora of manufacturing units that are facing the problem of erosive wear. Owing to the influence of abrasive along with hard particles employed in the components, which are utilised in hydro machinery causing erosion, the reduction of the efficiency of turbine frequently occurs, which ultimately halts whole working operations [1-2]. There are myriad factors, for instance, the size and hardness of erodent particles, level of slurry concentration, the impact velocity of abrasive particles as well as the target surface characteristics that influence the erosive wear of elements utilised in hydro machinery [3-7]. Turbines, propellers, pumps, and valves are the most commonly used components in fluid machinery. The equipment utilised in this machinery is generally made of cast iron, mild steel and stainless steel. These materials, on the other

hand, are much less resistant to erosive wear [8-9]. The development of novel erosion-resistant materials is important. Various techniques, including heat treatment and surface coatings, have been explored to make the surface hard to the impact of erodent particles in order to reduce erosion wear. The laser cladding technique has numerous advantages over traditional approaches, including strong adhesion between the deposition powder and the substrate, reduced heat involvement, and surface deformation, which need to be cladded. Due to significant advancements in technology along with science involved in lasers, material processing techniques using lasers [10,11] have been considered a favoured technique for the treatment of the surface. In comparison to conventional approaches, surface treatments done by laser processing techniques have shown improved surface hardening of the material, fatigue, reduction in the erosion and corrosion rate, as well as reduction of stress corrosion along with the elimination of cracks, which are most common during other surface treatments, of distinct alloys and metals [10,11]. Savanth *et al.* [12] deposited the Colmonoy-5 coatings on medium carbon steel by the laser cladding technique by varying the laser cladding parameters such as laser beam power and scanning speed. With the help of laser cladding, there was a strong metallurgical bond between the substrate and coating. The hardness of the coating has been increased with an increase in the laser cladding as that of the scanning speed. The sound cladding has been obtained and laser power had more influence on the hardness than of scanning speed. Moskal *et al.* [13] analysed the characterization of the primary microstructure of laser-cladded NiCrAlY coatings deposited on Inconel 625 Ni-based superalloy and 316L stainless steel. It was found that the dendritic microstructure was the result of rapid solidification due to differences in the chemical composition of dendritic and inter-dendritic areas. Paul *et al.* [14] used the laser cladding approach and deposited two powders, namely, Metco-41C and NiCrSiBC and coatings produced by this technique were found to be crack-free. Yao *et al.* [15] produced TiN/Al composite coating and after the deposition of coating powders, there was a significant improvement in wear as well as the micro-hardness. The reason was an increase in the count of narrow and elongated dendrites in the cladded surfaces. Thus, the laser cladding method as a surface treatment should be investigated to improve the erosion problem in hydro machinery components.

On the paradoxical side, in the last few decades, plenty of researchers used distinct powders such as nickel-based, iron-based, tungsten carbide-based and cobalt-based powders in many industrial applications to enhance the characteristics of different materials [16]. Nickel-based and WC powders have received the most interest as wear-resistant coatings [16]. Nickel-based powders exhibit a number of desired features that make them feasible to use in a variety of prospective engineering purposes [17], including strong bonding strength, improved corrosion behaviour, and great resistance to wear owing to adhesive and abrasive mode of failure. In addition, WC-cladded coating offers a lot of potential by virtue of qualities such as high hardness, enhanced resistance to wear, coefficient of thermal expansion is low, and good plasticity [18-21]. In order to attain sound carbide composite coating, Fishman *et al.* [22] used a laser cladding approach to manufacture WC coating on high-speed steel. The coatings, single layers produced with 40-50 percent WC, had hardness in the range of 1100–1200 HV9.81N. Yang *et al.* [23] created laser clads on the target surface of AISI 1010 steel using a blend of WC/Co powders and reported that the wear resistance was improved over the base material. Hence, in the current study, Colomonoy-6+WC coatings have been deposited on SS304 and SS410 steels using the technique of laser cladding. Further, cladded steels are used for the analysis of micro-hardness, porosity, microstructure and slurry erosion. A comparison of the mass loss owing to the slurry of Colmonoy-6+WC coated as well as uncladded

SS304 and SS410 steels was also conducted. Furthermore, the mechanism behind the wear of eroded surfaces has been investigated.

Experimental

Materials

The aim of the present study is to produce Ni-based and WC coatings on the SS304 and SS410 steels and evaluate their performance against slurry erosion. Samples of both above-mentioned steels were made. Specimens of 25 mm diameter and 7 mm width were made from the steel rod of 25 mm. Before the deposition of coatings, the surface of the target specimens was finished to remove the contaminants with the assistance of a surface grinder. Table 1 and Table 2 show the chemical composition of SS304 and SS410 steels as determined by spectroscopic analysis, as well as the ASTM standard composition [24,25]. The chemical composition of SS304 and SS410 steels, as determined by spectroscopy, is consistent with the ASTM standard. Owing to the presence of chromium and nickel, steel provides resistance to wear and corrosion.

Table 1. *The chemical composition of SS410 steel*

Component	Content, wt.%						
	Cr	C	S	Mn	P	Si	Fe
ASTM	11.5 to 13.5	<0.15	<0.03	<1	<0.04	<1	Balance
Untreated	11.857	0.1307	0.0249	0.9401	0.0319	0.9881	Balance

Table 2. *The chemical composition of SS304 steel*

	Content, wt.%								
Components	Cr	C	S	Mn	P	Si	Ni	N	Fe
ASTM	17.5 to 19.50	<0.03	<0.015	<0.045	<0.045	<1.0	8.00 to 10.50	.10	Balance
Untreated	17.928	0.028	0.012	1.469	0.0319	0.9814	8.91	.095	Balance

Laser cladding set up

The process of deposition of coatings was done at M/S Magod Laser Technologies, situated in Pune, India, with the diode laser cladding setup. A diode laser (LASERLINE, LDF 4.000, Germany) system has a special feedings system, which is coaxial in function, a beam delivery system, and a five-axis workstation provides more flexibility. The cladding material on the substrate was Colmonoy-6 +WC powder, and the properties of its elements [26,27] are listed in Table 2. As illustrated in Figure 1, a scanning electron microscope (SEM) JEOL, JSM6510LV has been utilized in order to investigate the structure and shape of the coating powder particles. The Colmonoy-6 particles had a spherical shape, as shown in SEM images, but the shape of WC particles was found to be elongated. Prior to laser cladding, Colmonoy-6 and WC powder were combined in an equivalent amount (50 wt.%) utilising a blending method. A double cone blender (ILDCB001, Innovative Engineering Work, India) was employed for optimum blending. Powders were then put into the powder feeding mechanism. A diode laser with a coaxial powder feeding system was used to clad the steel specimens with a laser beam. The powders created from the double cone blender, which blended the Colmonoy-6+WC powders, were fed into the powder feeding system's bin. The powder feed system allows for a consistent flow of powder in a stream with a diameter of 2 mm and a flow rate of powder ranging from 10-40 g min^{-1}. The purpose of shielding and carrier gas is done by argon. Earlier, the aim of removing all contaminants from the substrate's surface was done by sandblasting, which involved grit blasting the substrate with alumina (Al_2O_3), and after the

sandblasting, the surface was washed with de-ionized water along with acetone. There is a need for required surface roughness (7-9 µm) for producing the sound coating adhesion and this process was done through sandblasting [28]. As indicated in Table 3, steels were cladded using the laser cladding technique at optimal levels of several process parameters, namely: scanning speed, laser power, and powder feed rate. It was discovered that the above-mentioned laser cladding process parameters (scanning speed to be 1700 mm min^{-1}, laser power to be 2000 W, powder feed rate to be 30 g min^{-1}) were optimal for producing sound coating and illustrated in Table 4 [29].

Table 3. *Properties of powders (tungsten carbide and Colmonoy-6)*

Name of Powder	Density, g/cm^3	Melting point, °C	Hardness, Rockwell C scale
Colmonoy-6	8.10	1030	56-61
Tungsten carbide	10.0	2785-2830	88+

Table 4. *Process parameters used during laser cladding*

Process parameters	Range
Laser power, kW	2
Scanning speed, mm min^{-1}	1700
Powder feed rate, g min^{-1}	30

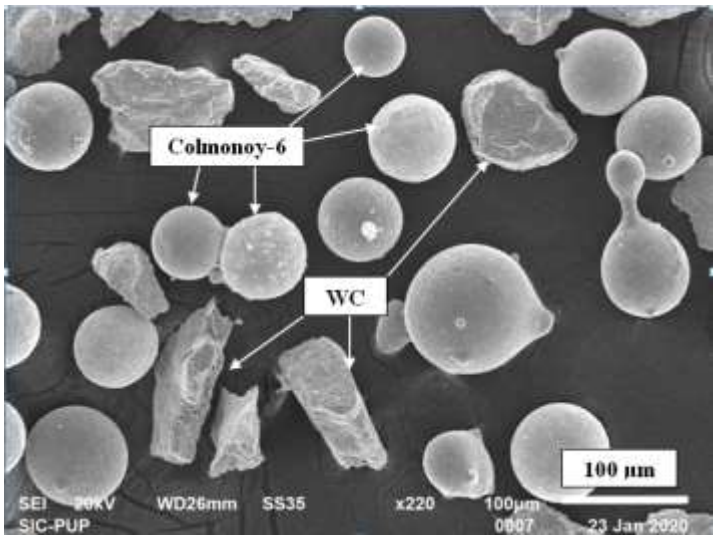

Figure 1. *SEM micrograph of Colmonoy-6+WC powder*

Mechanical and material characterization of treated and untreated specimens

For micro-hardness testing, the grit size of emery paper was from P100 to P1500 and used to polish the laser-clad and uncoated specimens. A Vickers microhardness tester (RMHT- 201, Radical Scientific Equipment Pvt. Ltd., India) has been used to assess the changes in cross-sectional micro-hardness of the Colmonoy-6+WC coatings under a 1 kg load and a 25-seconds dwell period. In addition, the space between two consecutive indentations was maintained at 0.1 mm. Micro-hardness measurements were calculated as the average of twelve readings made in similar areas. SEM analysis was utilised to study the splat distribution and porosity of the polished coated samples in cross-section. Surface SEM micrographs were utilized to analyse the vivid porosity of cladded materials surface using Envision 3.0 Series image analyser software (Chennai Metco Private Limited, India). Furthermore, SEM has been utilized to analyse the slurry erosion performance of laser cladded and uncoated specimens.

Slurry preparation

Natural sand has been employed as striking material in the experimental investigation of slurry erosion, and its morphology is depicted in Figure 2. The shape of sand particles is uneven, with sharp edges, as shown in the SEM image. Larger silt particle sizes over 800 are unable to access the hydraulic components due to the existence of sedimentation chambers and sand filters and are thus excluded for erosion testing. Therefore, an average particle size of 350 µm is used for the current study.

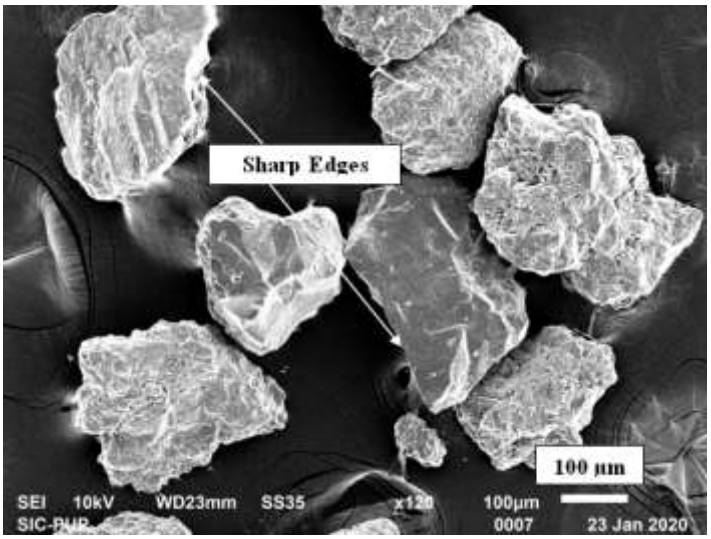

Figure 2. *SEM image of erodent sand particles*

Slurry erosion analysis

Slurry erosion experimentation was conducted at various variables using a specifically manufactured test rig, as depicted in Figure 3 and the same had been utilized in previous work [29].

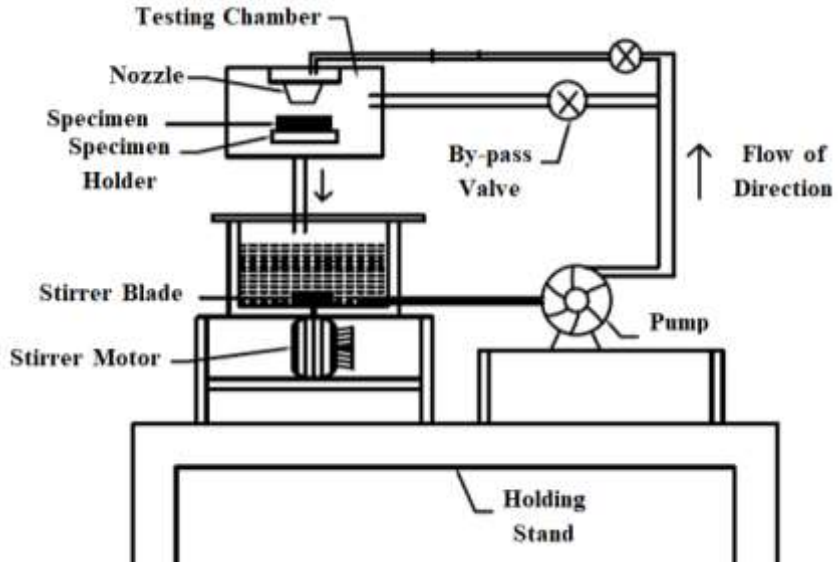

Figure 3. *Schematic diagram of the slurry erosion test rig*

The influence of two factors, impact velocity of erodent particle and impact angle, were investigated. Clad specimens were kept within the testing chamber in the specimen holder and had the capacity to adjust the orientation of the target surface in order to study the impact angle effect. A nozzle directs the combination of erodent particles and water in the testing chamber. A rotating vane pump is installed at the bottom, and one end of the pump is used to carry the slurry from the mixing chamber and directs the flow to the nozzle. There are valves built in the delivery pipe in order to

control the amount and pressure of the slurry. The slurry concentration is prepared in the mixing chamber with a predefined sand particle size, as required by the test and for present experimentation, the slurry concentration is 35,000 ppm. In order to avoid the settlement of erodent particles at the bottom, a stirrer is used in the mixing chamber. The mass loss was calculated at regular intervals by a precision microelectronic balance (ME36S, Cubis Laboratory Balances) and the accuracy of this machine is 0.1 mg. The diameter of the nozzle and the distance between the nozzle and target surface were set at 5 mm and 2.8 cm, correspondingly.

As per ASTM standard G-73 [30], erosive wear analysis has been done on uncladded and cladded steel specimens. Moreover, the levels of the parameters mentioned above have been considered are illustrated in Table 3. Impact angles can be adjusted by moving the specimen holder around to examine the influence of impact angles of erodent particles. Myriad investigations have determined that ductile materials exhibit the most erosion at 20-40º impact angles, while materials that are brittle in nature exhibit the most erosive wear at 90° [31-34]. As a result, impact angles of 30 and 90° were chosen for slurry erosion experimentation. Most of the time, the relative velocity between the slurry and impeller varied between 10 and 35 m s^{-1} [35,36]. As a response, two levels of impact velocity (15 and 30 m s^{-1}) were considered in the slurry erosion testing to imitate real-world conditions. In order to analyse the impact of both variables, full factorial was used, as represented in Table 5. Slurry erosion testing was done for one hour. Table 6 represents slurry erosion testing using a full factorial array and these combinations have been used for the slurry erosion testing. According to the slurry erosion tests, the cladded specimens had a lower rate of erosion than uncladded specimens. After each hour of testing, the mass loss was computed, and in order to measure accurate measurement, the process of cleaning the specimens with acetone was done before the measurement of mass loss. SEM images were used to examine the eroded specimens in order to understand the actual mechanisms that cause slurry erosion.

Table 5. *Different levels of slurry erosion parameters*

S. No.	Velocity, m s^{-1}	Impact angle, º
1	15	30
2	30	90

Table 6. *Slurry erosion testing using a full factorial array*

	Velocity, m s^{-1}	Impact angle, º
Test 1	15	30
Test 2	15	90
Test 3	30	30
Test 4	30	90

Results and discussion

Characteristics of coating deposition

Figure 4 represents SEM images of the cross-section surface of laser-clad SS304 and SS410 steels, respectively. From the cross-sectional SEM images, the coating had a metallurgical connection between the coating and substrate. Though there were fewer microvoids owing to the porosity of cladding materials, the coating seemed to have fewer defects. The value of porosity obtained for the coatings was in the range between 1.3 and 1.6 % (in both steels), and the same values were reported by different researchers with the deposition of the same cladded materials [21]. According to the

cross-section SEM images, the thickness, which was higher than 1 mm, was observed for the coating. From the SEM images, it was witnessed that carbides were evenly dispersed in Colmonoy-6 pool. Although most of the carbides were spherical in shape, on the surface, a few unevenly shaped carbides were detected.

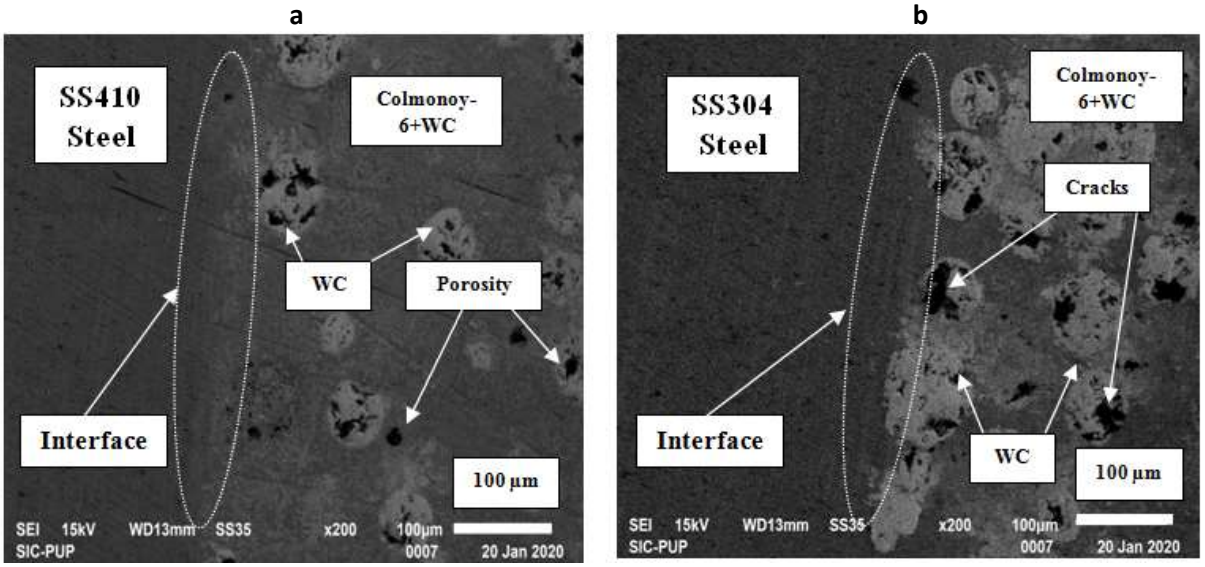

Figure 4. *(a) Cross-sectional SEM image of laser cladded SS410 steel and (b) cross-sectional SEM image of laser cladded SS304 steel*

The hardness of the uncoated SS304, SS410 steel, and cladded steels was represented in Figure 5. The value of hardness was measured at a distinct position on the cladding top surface with the application of 1 kg. The hardness of cladded surface was much higher than the substrate materials. The average hardness of SS304 and SS410 steel was noticed to be 152 and 178 $HV_{9.81N}$, respectively. An increase in microhardness was seen after the cladding of Ni+WC-based coatings on both steels, which could be related to the presence of dispersed carbides on the cladded surfaces [37]. The coating's micro-hardness ranged from 1009 to 1113 $HV_{9.81N}$, with a mean value of 1074 $HV_{9.81N}$ in the case of SS304 steel and 1079 $HV_{9.81N}$ for SS410 steel. This represents that after the coating deposition, there is no remarkable impact on the base material and hardness, found to be almost the same in both cladded surfaces.

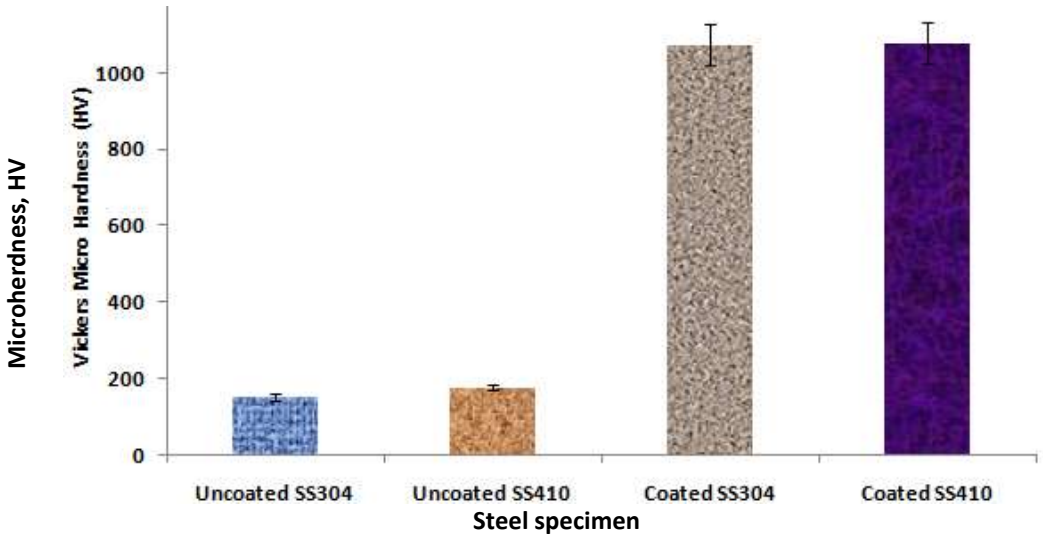

Figure 5. *Micro-hardness of coated and uncoated steel specimens*

Mechanism of slurry erosion

Experimental investigations of slurry erosion were carried out on the above-mentioned cladded material and uncladded steel specimens under various operating circumstances. As indicated in Figure 6, the bar graph elucidates the information regarding the change in mass loss of cladded and uncladded specimens. When comparing uncoated SS410 and SS304 steels to Colmonoy-6 + WC-cladded steel, it was discovered that the latter had stronger resistance to erosion. This could be due to the higher clad surface's hardness compared to uncladded steels. The maximum erosion was at the maximum impact velocity (30 m s^{-1}). The reason for this, when the impact velocity increases then, there is also an increase in the kinetic energy of sand particles. Consequently, maximum mass loss was noticed in all experiments. Goyal *et al.* [38] carried out the research work on slurry erosion analysis of steel and it has been observed that impact velocity was the major contributor to slurry erosion and similar results have been reported by Lopez *et al.* [39]. Further, utmost erosion was observed at an angle of 30° and this represents the ductile failure and as the impact angle increases, this exhibits more resistance to erosion owing to the brittle mode of failure [40-42].

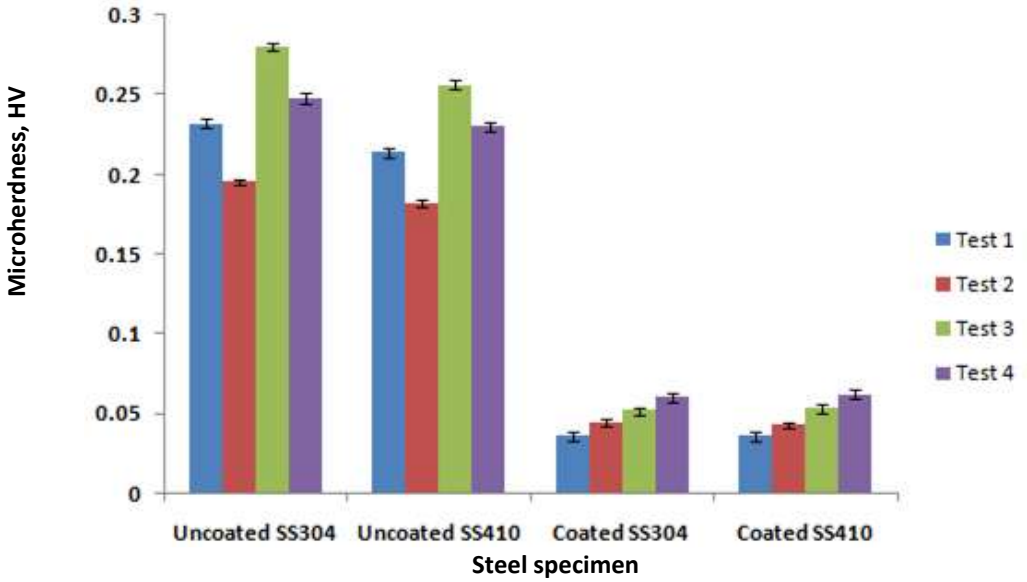

Figure 6. *Loss of mass after erosion of laser-cladded and uncoated SS304 and SS410 steel using 4 mm jet*

Eroded surface analysis

Most of the time, the mechanism of removal of material under slurry erosion is affected by the properties of encountered surfaces of the material and working parameters in general [38]. Plastic deformation, along with cutting, is used to erode the material from the target surface in the case of the ductile mode of wear [43]. Fatigue failure occurs in brittle materials when energy is transferred to the target surface of the material by the repetitive influence of erodent particles [38]. Furthermore, distinct erosion mechanisms exist for different operating situations, such as low plus high impact angles, and for the lower impact angles, ploughing, chip formation, and cutting are the mechanisms which are generally occurred on eroded surfaces [44]. Cracks and craters formed by material erosion as platelets, on the other hand, are plausible erosion mechanisms for normal impact [45]. The subsequent paragraphs illustrate the erosion mechanisms of cladded and uncladded steel specimens.

Uncoated SS304 and SS410 steel

After the polishing of as received steels before erosion causes some scratches on the surface. SEM images of uncoated steels after the erosive wear occurred at using impact angle of 30° and

impact velocity of 30 m s^{-1}, are shown in Figure 7. Maximum erosion has been witnessed in the case SS304 steel as that of SS410 steel. This is because of the higher hardness of SS410 steel against the SS304 steel. At this operating condition, slurry erosion was found to be highest as with a higher impact angle, the more mass removal rate was noticed, and the mode of failure in both cases was ductile. Steel surface had some cracks and the same was represented in Figure 7, which paved the way to the continuous and normal impact of erodent particles, while on the eroded surfaces of steel specimens, lip formation was seen, which could be related to the ductile mode of failure of the material under higher erodent particle velocity (30 m s^{-1}) and low impact angle (30°) [45]. Signatures of the ploughing and micro-cutting have been observed on the eroded surface of steel, as illustrated in SEM pictures, may be caused by the same mechanism. Further, it also has been witnessed that the wear resistance of SS410 is more owing to the higher hardness, and that is the reason there is less plastic deformation in comparison with SS304.

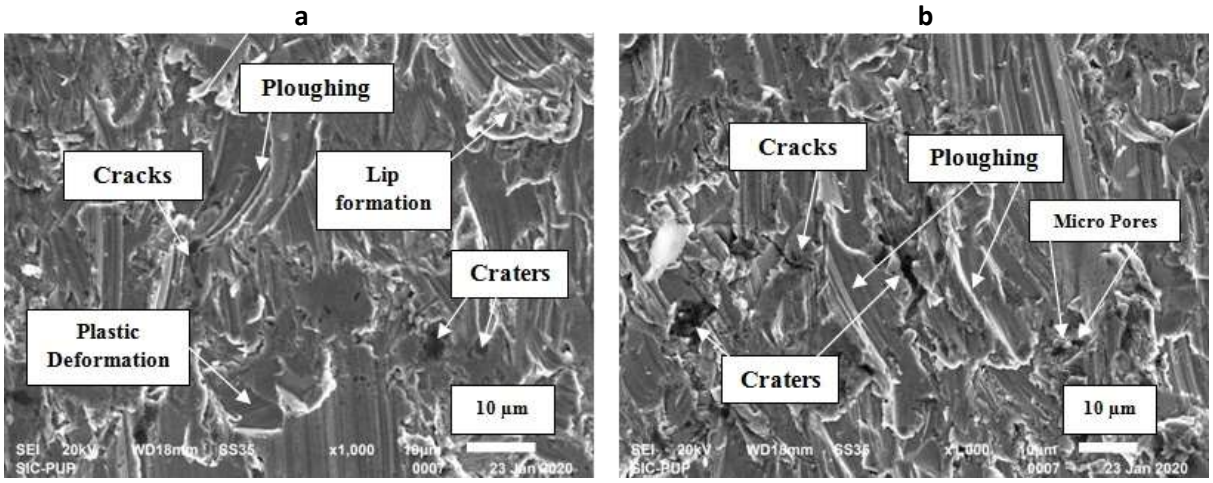

Figure 7. *SEM images of (a) uncoated SS304 steel and (b) uncoated SS410 steel after erosion*

Coated SS304 and SS410 steel

Figure 8 shows SEM images of cladded SS304 and SS410 steel after the maximal rate of wear at the velocity of 30 m s^{-1} and 90° impact angle.

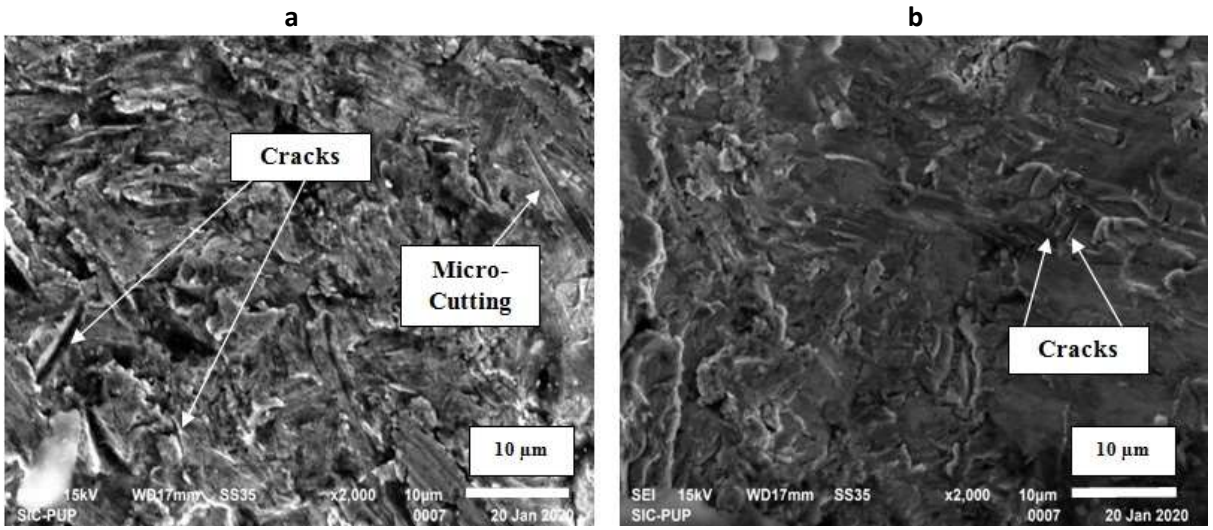

Figure 8*. SEM images of (a) coated SS304 steel and (b) coated SS410 steel after erosion*

A significant number of cracks were created on the eroded cladded surface by dint of the continuous impact of erodent particles at 90°. After the deposition of cladded powder, a significant

increase in wear resistance was noticed and the mode of failure was brittle because there was no formation of lip, ploughing and crater. The reason behind this mode of failure is owed to the impact angle of 90°. T. Savanth *et al.* [12] evaluated the slurry erosion performance of Colomonoy-5; it was found that under the same operating conditions, the mode failure was brittle, which was in accordance with the present research work. Further, research work carried out by Paul *et al.* [14] was on the slurry erosion performance of laser cladded 316 L steel and it was found that the mode of failure was brittle. Moreover, the mode of failure was almost the same in the case of coated SS304 and SS410 steels and no significant effect of the base material was observed.

Conclusions

- The laser cladding technique was used to successfully create Colmonoy-6+ WC coatings on SS304 and SS410 steels under specified laser cladding process parameters: scanning speed, laser power and powder feed at 1700 mm/s, 2 kW and 30 g/min, respectively.
- There was a significant improvement in hardness after the deposition of coating materials. The hardness of the cladded steels was found to be more than six times of the uncladded steel specimens.
- Mass loss was found to be less in the coated specimens than in the uncladded specimens. The reason behind this was the higher hardness of the deposited coating. The most significant factor for mass loss of coated and uncladded steel was found to be impact velocity.
- Signs of lip formation, craters, ploughing were observed in the case of eroded uncoated steel specimens and the mode of failure was ductile, while the eroded cladded specimens had no signs of lip formation and ploughing. Owing to the brittle mode of failure, there were some cracks on deposited coatings.

References

[1] A. Bansal, J. Singh, H. Singh, *Journal of Thermal Spray Technology* **7** (2019) 1448-1465. https://doi.org/10.1007/s11666-019-00903-y
[2] Q. B. Nguyen, C. Y. H. Lim, V. B. Nguyen, Y. M. Wan, B. Nai, Y. W. Zhang, M. Gupta, *Tribology International* **79** (2014) 1-7. https://doi.org/10.1016/j.triboint.2014.05.014
[3] V. Singh, I. Singh, A. Bansal, A. Omer, A. K. Singla, D. K. Goyal, *Surface and Coatings Technology* **432** (2022) 128052. https://doi.org/10.1016/j.surfcoat.2021.128052
[4] M. A. Al-Bukhaiti, S. M. Ahmed, F. M. F. Badran, K. M. Emarab, *Wear* **262** (2007) 1187-1198. https://doi.org/10.1016/j.wear.2006.11.018
[5] M. M. Stack, T. M. Abd El-Badia, *Wear* **264** (2008) 826-837. https://doi.org/10.1016/j.wear.2007.02.025
[6] R. Dasgupta, B. K. Prasad, A. K. Jha, O. P. Modi, S. Das, A. H. Yegneswaran, *Materials Transactions* **39** (12) (1998) 1185-1190. https://doi.org/10.2320/matertrans1989.39.1185
[7] A. K. Jha, R. Batham, M. Ahmed, A. K. Majumder, O. P. Modi, S. Chaturvedi, A. K. Gupta, *Transactions of Nonferrous Metals Society of China* **21** (2011) 32-38. https://doi.org/10.1016/S1003-6326(11)60674-2
[8] A. Bansal, D. K. Goyal, P. Singh, A. K. Singla, M. K. Gupta, N. Bala, J. Kolte, G. Setia, *International Journal of Refractory Metals and Hard Materials* **92** (2020) 105332. https://doi.org/10.1016/j.ijrmhm.2020.105332
[9] A. Bansal, J. Singh, H. Singh, *Wear* **456** (2020) 203340. https://doi.org/10.1016/j.wear.2020.203340
[10] B. L. Mordike, *Progress in Material Science* **42** (1997) 357-372. https://doi.org/10.1016/S0079-6425(97)00024-8

[11] S. Kalainathan, S. Sathyajith, S. Swaroop, *Optics and Lasers in Engineering* **50** (2012) 1740-1745. https://doi.org/10.1016/j.optlaseng.2012.07.007
[12] T. Savanth, J. Singh, J. S. Gill, *Proceedings of the Institution of Mechanical Engineers*, *Part L: J. Materials: Des. Appl.* **234(7)** (2020) 947-961. https://doi.org/10.1177/1464420720922568
[13] G. Moskal, D. Niemiec, B. Chmiela, P. Kalamarz, T. Durejko, M. Zietala, T. Czujko, *Surface and Coatings Technology* **387** (2019) 125317. https://doi.org/10.1016/j.surfcoat.2019.125317
[14] C. P. Paul, B. K. Gandhi, P. Bhargava, *Journal of Material Engineering and Performance* **23** (2014) 4463-4467. https://doi.org/10.1007/s11665-014-1244-9
[15] F. Yao, X. C. Zhang, J. F. Sui, S. T. Tu, F. Z. Xuan, Z. D. Wang, *Optics and Laser Technology* **67** (2015) 78–85. https://doi.org/10.1016/j.optlastec.2014.10.007
[16] S. Singh, D. K. Goyal, P. Kumar, A. Bansal, *Material Research Express* **7(1)** (2020) 012007. https://doi.org/10.1088/2053-1591/ab6894
[17] : J. Mazumder*, Laser assisted surface coatings* in: *Metallurgical and Ceramic Protective Coatings*, K.H. Stern (Ed.), Springer, Dordrecht, 1996, pp.74-111. https://doi.org/10.1007/978-94-009-1501-5_5
[18] A. Pascu, H. Iosif, T. Mircea, H. Croitoru, C. Stanciu, E. Manuel, R. I. Claudiu, *Engineering Science* **254** (2016) 77-82. https://doi.org/10.4028/www.scientific.net/SSP.254.77
[19] Z. Chen, L. C. Lim, M. Qian, *Journal of Materials Processing Technology* **62** (1996) 321-323. https://doi.org/10.1016/S0924-0136(96)02428-4
[20] P. Wu, H. M. Du, X. L. Chen, Z. Q. Li, H. L. Bai, E. Y. Jiang, *Wear* **257** (2004) 142-147. https://doi.org/10.1016/j.wear.2003.10.019
[21] K. V. Acker, D. Vanhoyweghen, R. Persoons, J. Vangrunderbeek, *Wear* **258** (2005) 194–202. https://doi.org/10.1016/j.wear.2004.09.041
[22] M. Riabkina-Fishman, E. Rabkin, P. Levin, *Materials Science and Engineering A* **302** (2001) 106–114. https://doi.org/10.1016/S0921-5093(00)01361-7
[23] M. Zhong, W. Liu, Y. Zhang, X. Zhu, *Surface and Coatings Technology* **24(6)** (2006) 453-460. https://doi.org/10.1016/j.ijrmhm.2005.09.002
[24] A. Bansal, A. K. Singla, V. Dwivedi, D. K. Goyal, J. Singla, M. K. Gupta, G. M. Krolczyk, *Journal of Manufacturing Processes* **56** (2020) 43-53. https://doi.org/10.1016/j.jmapro.2020.04.067
[25] E. Bringas, *Handbook of comparative world steel standards West Conshohocken*, Montgomery County, Pennsylvania, United States, Third edition, ASTM International, 2004. http://lccn.loc.gov/2015042235
[26] P. Farahmand, T. Frosell, M. McGregor, R. Kovacevic, *The International Journal of Advanced Manufacturing Technology* **79** (2015) 1607–1621. https://doi.org/10.1007/s00170-015-6936-2
[27] A. Milionis, E. Loth, I. S. Bayer, *Advances in Colloid and Interface Science* **229** (2016) 57-79. https://doi.org/10.1016/j.cis.2015.12.007
[28] G. R. Desale, C. P. Paul, B. K. Gandhi, S. C. Jain, *Wear* **266** (2009) 975-987. https://doi.org/10.1016/j.wear.2008.12.043
[29] S. Singh, D. K. Goyal, P. Kumar, A. Bansal, *International Journal of Refractory Materials and Hard Metals* **105** (2022) 105825. https://doi.org/10.1016/j.ijrmhm.2022.105825
[30] H. Singh, K. Goyal, D. K. Goyal, *Manufacturing Science and Technology* **2(4)** (2014) 81-92. https://doi.org/10.13189/mst.2014.020403
[31] I. Finnie, *Wear* **186-187** (1995) 1-10. https://doi.org/10.1016/0043-1648(95)07188-1
[32] I. Finnie, *Wear* **3(2)** (1960) 87-103. https://doi.org/10.1016/0043-1648(60)90055-7
[33] D. K. Goyal, H. Singh, H. Kumar, *Journal of Engineering Tribology* **225** (2011) 1092-1105. https://doi.org/10.1177/1350650111412443
[34] H. Singh, K. Goyal, D. K. Goyal, *Transactions of the Indian Institute of Metals* **70** (2017) 1585-1592. https://doi.org/10.1007/s12666-016-0956-y

[35] *C. R. I. Pumps, Borewell submersible pumps series,* https://in.crigroups.com/products/agriculture-pumps Accessed 24/04/2022
[36] *D. Crompton greaves consumer electricals limited, Residential pumps: A6, A14, and A15 pumps catalogue*, https://www.crompton.co.in/p roduct-category/consumer-pumps/residential pumps Accessed 24/04/2022
[37] S. Singh, P. Kumar, D. K. Goyal, A. Bansal, *International Journal of Refractory Metals and Hard Materials* **98** (2021) 105573. https://doi.org/10.1016/j.ijrmhm.2021.105573
[38] D. K. Goyal, H. Singh, H. Kumar, V. Sahni, *Wear* **289** (2012) 46-57. https://doi.org/10.1016/j.wear.2012.04.016
[39] D. Lopez, J. P. Congote, J. R. Canob, A. Torob, A. P. Tschiptschin, *Wear* **259** (2005) 118-124. https://doi.org/10.1016/j.wear.2005.02.032
[40] G. T. Burstein, K. Sasaki, *Wear* **240** (2000) 80-94. https://doi.org/10.1016/j.wear.2014.08.006
[41] I. Finnie, G. R. Stevick, J. R. Ridgely, *Wear* **152** (1992) 91-98. https://doi.org/10.1016/0043-1648(92)90206-N
[42] H. C. Lin, S. K. Wu, C. H. Yeh, *Wear* **249** (2001) 557-565. https://doi.org/10.1016/S0043-1648(01)00580-4
[43] D. W. Wheeler, R. J. K. Wood, *Wear* **258** (2005) 526-536. https://doi.org/10.1016/j.wear.2004.03.035
[44] A. Conde, F. Zubiri, J. Damborenea, *Materials Science and Engineering A* **334** (2002) 233-238. https://doi.org/10.1016/S0921-5093(01)01808-1
[45] G. F. Sun, Y. K. Zhang, M. K. Zhang, R. Zhou, K. Wang, C. S. Liu, K. Y. Luo, *Applied Surface Science* **295** (2014) 94-107. https://doi.org/10.1016/j.apsusc.2014.01.011